Coordinatively Unsaturated Cp*Ru Alkoxo Complexes. 16.[1] Addition Products Cp*Ru(acac)L and Solution Equilibria[1]

U. Koelle,* C. Rietmann, and G. Raabe

Institute for Inorganic Chemistry, Aachen Technical University, D-52056 Aachen, Germany

Received August 20, 1996[⊗]

With $[Cp^*Ru(OMe)]_2$ (**1**) as starting material, a number of 2,4-pentanedionato complexes Cp*Ru(2,4-pentanedionate) were prepared. The solid-state structure of Cp*Ru(1-phenyl-2,4-pentanedionate) (**3**) was elucidated by X-ray crystallography, and the complex was found to be a dimer in the solid state, as previously established for Cp*Ru(2,4-pentanedionate) (**2**). The molecular weight of **3** in benzene indicates a dimer (**3**-**3**) in solution as well. Low-temperature ^{1}H NMR spectroscopy reveals a process involving dissociation of the dimer into monomers associated with an inversion of the pentanedionate ligand at Ru. The activation energy ($E_a = 43.5 \pm 0.7$ kJ/mol, toluene-d_8) reflects the enthalpy of dissociation of the dimer. All dimers are easily cleaved with two-electron ligands L, resulting in the mononuclear complexes Cp*Ru(2,4-pentanedionate)L. Besides isolable complexes with L = phosphine, phosphite, and CO, labile adducts of the same composition with σ-S and N donor ligands (L = methyl *p*-tolyl sulfoxide, ethyl methyl sulfide, tetrahydrothiophene, diaza[2.2.2]-bicyclooctane, 3-cyanopyridine) were detected in solution by the influence of these ligands on the observed inversion barrier. With chiral or enantiotopic ligands diastereoselective adduct formation was observed.

Introduction

Coordinatively unsaturated transition-metal complexes are of principal interest to coordination chemistry, since those species are crucial to many substitution processes as well as being involved in the elementary steps in catalytic cycles. A particular class of such coordinatively unsaturated d^6-5 complexes are the Cp* and arene Ru dimers bridged by OR, SR, NR, and NR_2 groups, which, apart from the Cp ligand, are devoid of additional stabilizing π-acceptor ligands. Only the chemistry of $[Cp^*RuOR]_2$[2] (**1**) and $[Cp^*RuSR]_2$[3] has been studied in detail.

The complex Cp*Ru(acac) (**2**) was first synthesized in the hope of generating a monomeric analogue to **1**[4] but was later recognized to be a dimer in the solid state[5] (Scheme 1). The monomers are connected by a long (2.43 Å) bond between Ru and the central carbon of the acac ligand of a second Cp*Ru(acac) fragment, in the same way as has been found previously for $[Cp^*Rh(acac)]_2^{2+}$.[6] Chemically, however, **2** behaved as an unsaturated molecule being rapidly cleaved by e.g. phosphines to give the monomeric $Cp^*Ru(acac)PR_3$. In fact, these addition and cleavage reactions occur almost instantaneously and could not be followed kinetically at ambient temperature. To further elucidate the concept, we have synthesized a number of pentanedionate derivatives and studied their reactions with two-electron-donor ligands. In particular the benzyl derivative $Cp^*Ru(OC(CH_2Ph)CHC(Me)O)$ (**3**), featuring diastereotopic protons in the dimer, allowed a detailed study of solution equilibria by NMR.

Scheme 1. Preparation of Cp*Ru(acac) Complexes

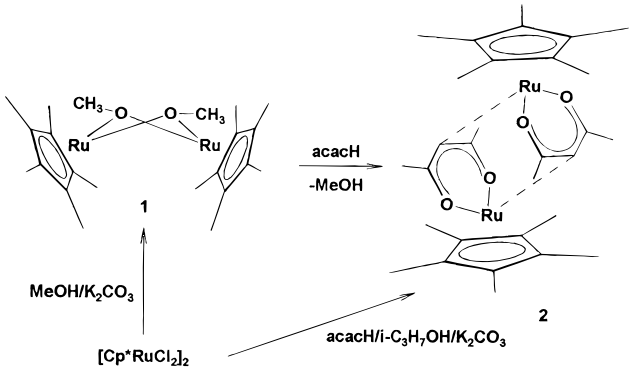

Results

Derivatives, Exchange, and Diastereoselectivity in Isolated Adducts. In addition to generation of **2** from **1** by exchange of the methoxo for the acac ligand,[4] we found a direct route to **2** from the dichloride $[Cp^*RuCl_2]_2$. The reaction is analogous to the preparation of **1** from the same material[2c] employing 2-propanol instead of methanol for reduction of Ru^{III}. Since 2-propanol does not act as a bridging ligand or is easily displaced by a pentanedionate, the reaction, carried out with a stoichiometric amount of acacH in the presence

[⊗] Abstract published in *Advance ACS Abstracts,* June 15, 1997.

(1) Part 15: Bücken, K.; Koelle, U.; Pasch, R.; Ganter, B. *Organometallics* **1996**, *15*, 3095.

(2) (a) Koelle, U.; Kossakowski, J. *J. Chem. Soc., Chem. Commun.* **1988**, 549. (b) Loren, S. D.; Campion, B. K.; Heyn, R. H.; Tilley, T. D.; Bursten, B. E.; Luth, K. W. *J. Am. Chem. Soc.* **1989**, *111*, 4712. (c) Koelle, U.; Kossakowski, J. *Inorg. Synth.* **1992**, *29*, 225.

(3) (a) Koelle, U.; Rietmann, C.; Englert, U. *J. Organomet. Chem.* **1992**, *423*, C20. (b) Takahashi, A.; Mizobe, Y.; Matsuzaka, H.; Dev, S.; Hidai, M. *J. Organomet. Chem.* **1993**, *456*, 243.

(4) Koelle, U.; Kossakowski, J.; Raabe, G., *Angew. Chem., Int. Ed. Engl.* **1990**, *29*, 773.

(5) Smith, M. E.; Hollander, F. J.; Andersen, R. A. *Angew. Chem.* **1993**, *32*, 1294.

(6) Rigby, W.; Lee, H. B.; Bailey, P. M.; McCleverty, J. A.; Maitlis, P. M. *J. Chem. Soc., Dalton Trans.* **1979**, 387.

S0276-7333(96)00718-2 CCC: $14.00

Chart 1. Diastereomeric Phosphine Adducts of Cp*Ru(PFBC)

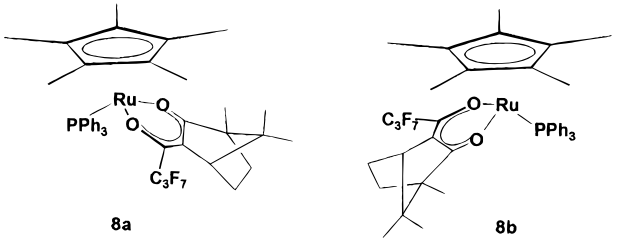

of a large excess of 2-propanol, gave the acac complex **2** in high yield. However, the method was less successful in the case of other pentanedionates, which were better prepared by methanol substitution from **1**. In this way Cp*Ru complexes (in some cases also C_5Me_4EtRu analogues) of 1-phenyl-2,4-pentanedionate (Phacac; **3**), benzoylacetonate (**4**), acetoacetic ester (**5**), diethyl malonate (**6**), 1,1,1-trifluoro-2,4-pentanedionate (**7**) and a 3-(perfluorobutyryl)camphor derivative (**8**) were obtained. The compounds are dull red, similar to **2**, and are air-sensitive in solution.

Two complexes, **6a** and **6b**, in the ratio 2:1 with slightly differing NMR shifts for all groups, were formed from **1** and diethyl malonate, which were both of composition $[Cp^*Ru(\text{diethyl malonate})]_n$ according to NMR and chemical analysis. The major isomer **6a** was easily cleaved with PPh_3 to give the mono(phosphine) adduct and is therefore believed to be a dimer with a structure analogous to **2**, whereas air-stable **6b** withstands cleavage and is most probably an oligomer where OEt groups are engaged in binding. The latter compound appears to be the thermodynamically more stable one, since all of the material was transformed into **6b** on recrystallization.

With phosphines, phosphites, and CO stable adducts of composition Cp*Ru(acac)L are formed with nearly all 2,4-pentanedionate ligands. An exception was found in the case of 2,2′-bipyridine, which cleaved one Ru−O bond in **2**, resulting in $Cp^*Ru(\eta^1\text{-OC(Me)CHC(Me)O})(\eta^2\text{-bpy})$. Similarly, **5** reacted with $P(OMe)_3$ to yield $Cp^*Ru(\eta^1\text{-OC(Me)CHCOOEt})(P(OMe)_3)_2$. NMR data for these adducts are given in Table 3.

When 1 equiv of PMe_3 was added to **3**·PPh_3, an instantaneous reaction was indicated by a deepening of the color. The NMR spectrum showed the formation of the PMe_3 adduct and the presence of 1 equiv of free PPh_3. Equilibrium 1 is thus shifted far to the right. Nevertheless, **3**·PMe_3 shows, different from **3**·PPh_3, a singlet for the benzylic protons at ambient temperature, indicating rapid dissociation in solution.

$$\mathbf{3}\cdot PPh_3 + PMe_3 \rightleftarrows + PPh_3 + \mathbf{3}\cdot PMe_3 \qquad (1)$$

$$\mathbf{3}\cdot PMe_3 \rightleftarrows \mathbf{3} + PMe_3$$

Using an acac-like ligand featuring diastereofaces such as D-(+)-3-(perfluorbutyryl)camphor (PFBC, whose Eu^{III} complex is used as a NMR shift reagent), two diastereomeric adducts Cp*Ru(PFBC)L are possible. In this particular case the primary reaction product Cp*Ru(PFBC) (**8**), obtained from **1** and PFBCH, was not easily separated from excess ligand. The PPh_3 adduct, however, could be purified, and integration of the Cp* doublets ($^4J_{PH}$ = 1.5 Hz) indicated a mixture of diastereomers in the ratio 1:0.12. Though we have no direct proof, it seems reasonable to assign structure **8a** to the major isomer.

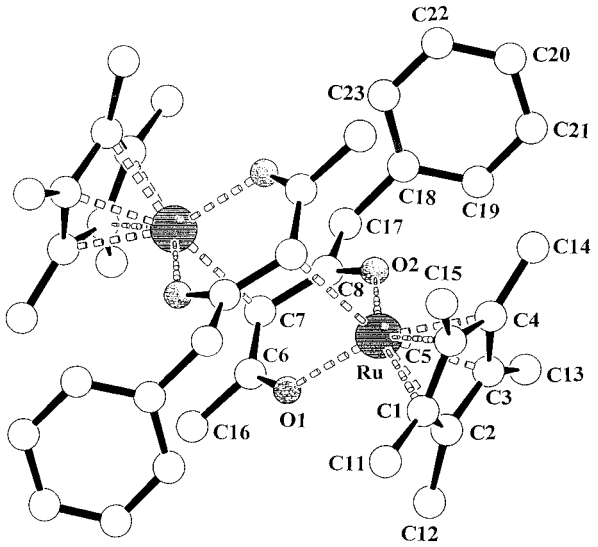

Figure 1. Schakal representation of the dimer **3-3**. Distances (Å) and angles (deg) are as follows: Ru−O2, 2.116(2); Ru−O1, 2.116(2); $Ru-C_{Cp}$(av), 2.127(3); Ru−C7′, 2.408; O1−Ru−O2, 85.32(6); Ru−O1−C6, 128.8(2); Ru−O2−C8, 128.4(2); O1−C6−C16, 115.9(2); O2−C8−C17, 126.1(2).

Composition and Structure of 3. The Phacac derivative **3,** due to its particular NMR spectroscopic properties, plays a key role in the present investigation and was therefore subjected to closer investigation. Osmometric molecular mass determination in benzene resulted in a value of 845 Da, consistent with a dimer (M = 822 Da). Determination of the solid-state structure revealed a molecular geometry (Figure 1) which largely conforms to the one found for **2**, i.e. a dimer formed from two centrosymmetrically related Cp*Ru(Phacac) units, connected by a Ru−C7 bond of length 2.408(3) Å. The O−Ru−O plane and the Ru−Cp* normal vector enclose an angle of δ = 36.5° (**2**, 37.4°). The plane O2−C6−C8−O3 is bent toward Ru by 5.5°. The same is true for carbon atom C7, which lies 0.2 Å below the plane O2−C6−C8−O3 and is shifted toward the metal atom of the opposing subunit. The Me group and the C8−C17 bond of the $PhCH_2$ group at the acac ring are also bent outwardly with respect to the acac plane and thus away from the metal. Bending of the acac ligand with respect to the Ru−Cp* normal vector is most likely due to the Ru−C7 interaction. To confirm this assumption, we performed nonempirical quantum-chemical calculations with the density functional method[7] on a model compound where the phenyl substituent at acac and the methyl groups of the Cp* system were replaced by hydrogen atoms. The calculations were carried out in the local approximation, employing a numerical basis set of approximately 6-31G** quality. Complete geometry optimization starting from the experimentally determined value of δ resulted in a final angle of about 6.5°. In the solid state the phenyl group within each subunit is bent toward the Cp* ligand with

(7) (a) *Biosym Dmol2.2 User Guide*; Bisoym Technologies: San Diego, CA, 1992. (b) Moruzzi, V. L.; Janak, J. F.; Williams A. R. In *Calculated Electronic Properties of Metals*; Pergamon Press: New York, 1978. (c) Hedin, L.; Lundqvist, B. I. *J. Phys. Chem.* **1971**, *4*, 2064.

Scheme 2. Enantiomers and Diastereomers of Cp*Ru(OC(CH$_2$Ph)CHC(Me)O)

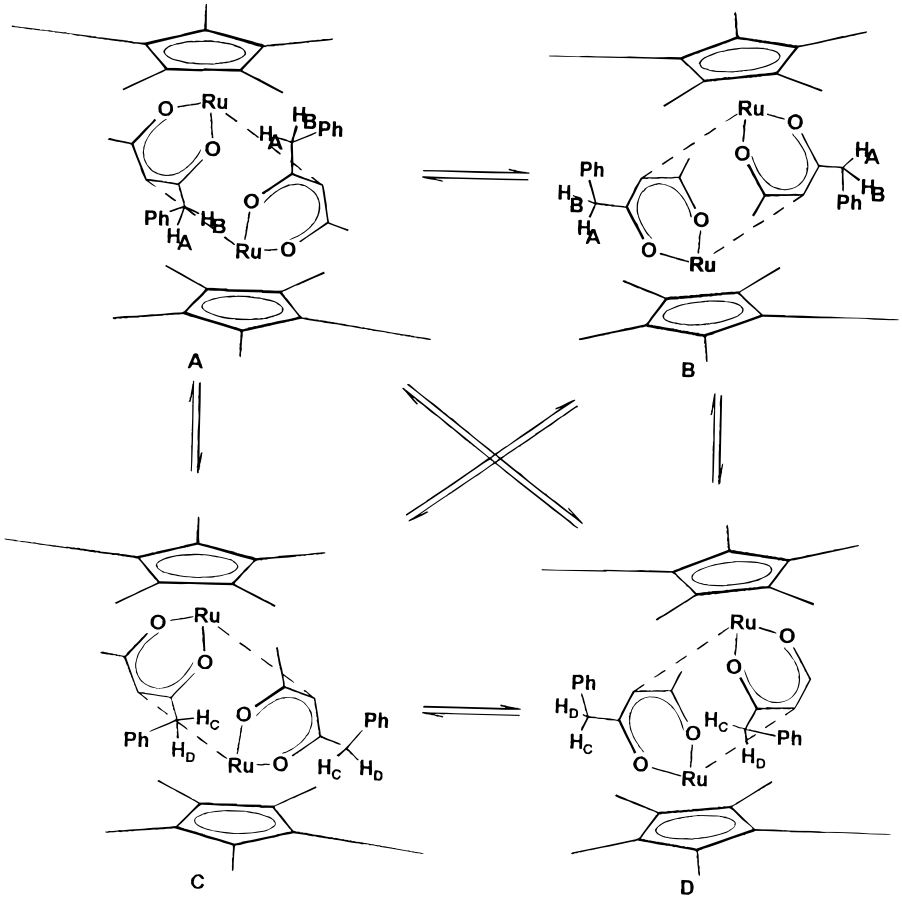

an O2−C8−C17−C18 dihedral angle of 18.5°. This conformation of the phenyl group is probably enforced by the opposite subunit or by packing forces of the lattice, because EHT calculations on the (bent) monomer result in energy minima of about −60 and 80° respectively.

Solvent-Dependent Variable-Temperature ^{1}H NMR Spectra of 3. The dimer **3-3** can exist in four isomeric forms, depicted in Scheme 2. They consist of two pairs of enantiomers arranged horizontally and two pairs of diastereoisomers arranged vertically. In the latter $PhCH_2$ groups are disposed *cis* and *trans* to each other. Interconversion of enantiomers A/B and C/D interchanges diastereotopic protons H_A/H_B and H_C/H_D and can thus be monitored by NMR. In addition, two separate signal sets due to diastereoisomers are to be expected in the slow-interconversion limit. Both horizontal and vertical processes require dissociation into monomers and should therefore show the same activation parameters.

Variable-temperature ^{1}H NMR spectra were recorded in CD_2Cl_2, in toluene-d_8 and in THF-d_8 at 400 and 500 MHz proton frequency. At ambient temperature benzylic protons appear as a singlet in all solvents. In CD_2Cl_2 the low-temperature spectrum (400 MHz) exhibits a sharp AB quartet for the benzylic protons which persists up to −10 °C. Above this temperature the complex starts to react irreversibly with the solvent to give unstable Cp*Ru^{III}(OC(CH$_2$Ph)CHC(Me)O)Cl as one of the products.

The singlet of the benzylic protons in toluene (δ 3.25) at room temperature starts broadening at −40 °C and has emerged as a seven-line pattern at −90 °C. This can be interpreted as two overlapping AB quartets of unequal intensity (labeled A and B in Figure 2). Concomitant with the splitting of the benzylic protons appears a splitting of the methyl group at C3 and also of the protons of the phenyl ring (fortunately well separated from residual solvent signals at low temperature). This was most noticeable for the ortho protons, which, at −90 °C, appear as *two* doublets instead of *one*. The overall pattern is attributed to the two dynamic processes of Scheme 2, which, at sufficiently low temperature, generate diastereomeric pairs with four dia-

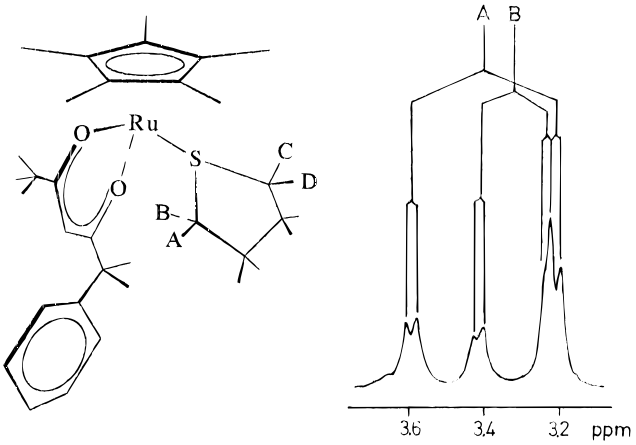

Figure 2. Part of the ^{1}H NMR spectrum of **3** in toluene-d_8 at −85 °C showing the benzylic proton signal pattern as two overlapping AB quartets of unequal intensity, labeled A and B.

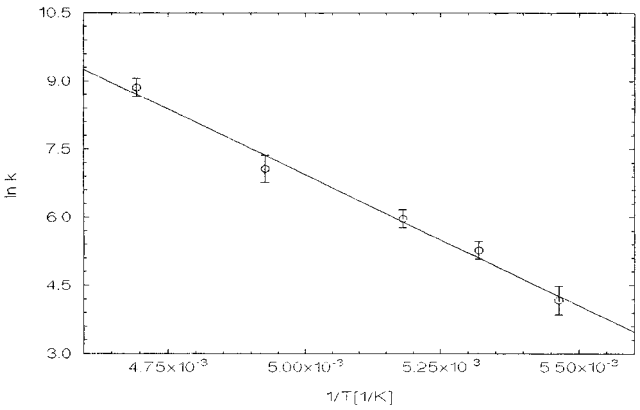

Figure 3. Arrhenius plot from the temperature-dependent line width of benzylic protons of **3**.

stereotopic benzylic protons H_A, H_B, H_C, and H_D in the form of two AB quartets with an intensity ratio of about 55:45.

Three interconversion barriers can be determined independently from VT NMR spectra by monitoring the coalescence of the AB quartets, the methyl singlets, and the ortho proton doublets. Fitting the line shape to the coalescing AB quartets by varying the rate constant k as well as the ratio of diastereoisomers led to the Arrhenius plot given in Figure 3 with an apparent value of $E_a = 43$ kJ/mol. The activation energy obtained for the interconversion of ortho phenyl protons is close enough to this value to consider the processes responsible for the two spectral changes as being concerted, that is identical, and reflect opening and recombination of the dimer. To investigate the adduct equilibria discussed below, in any particular case the most convenient of these spectral changes was chosen to follow inversion of the acac ligand.

In THF only a slight broadening without splitting into separate signals was observed down to the lowest accessible temperature of about −100 °C.

The largely differing inversion barriers (interconversion of enantiomers corresponds to an inversion at Ru) in the three solvents must be interpreted as different stabilization of the monomer. From a beginning line broadening at −10 °C in dichloromethane the barrier ≥60 kJ/mol ($\Delta G^{\ddagger}$) is estimated, at least 30 kJ/mol higher than in toluene (Table 2). In contrast, a considerably lower barrier (if any) follows from LT NMR in THF. A specific stabilization of the monomer by addition of CH_2Cl_2, the same as has been found for the isoelectronic $CpRe(NO)(PPh_3)^+$,[8] is the logical explanation for the persisting AB quartet in this solvent. Stabilization of the monomer by toluene seems to be less pronounced, and therefore, the complex in this solvent is dimeric, as it is in the solid state. A possible explanation for the rapid interconversion in THF is a solvent-stabilized monomer in this solvent as well. However, dissociation must be much faster in the THF than in the dichloromethane adduct.

Adduct Formation Equilibria. In order to gain more insight into the adduct-forming capabilities of **3** (or **2**, respectively), the above interconversion process was modulated by addition of a variety of ligands L ranging from π-acceptor to weak σ-donor. Isolable adducts are formed with CO and PPh_3; adduct formation with the other bases was detected by a shift of NMR signals and by the influence on NMR barriers.

Scheme 3. Adduct Formation and Inversion of 3

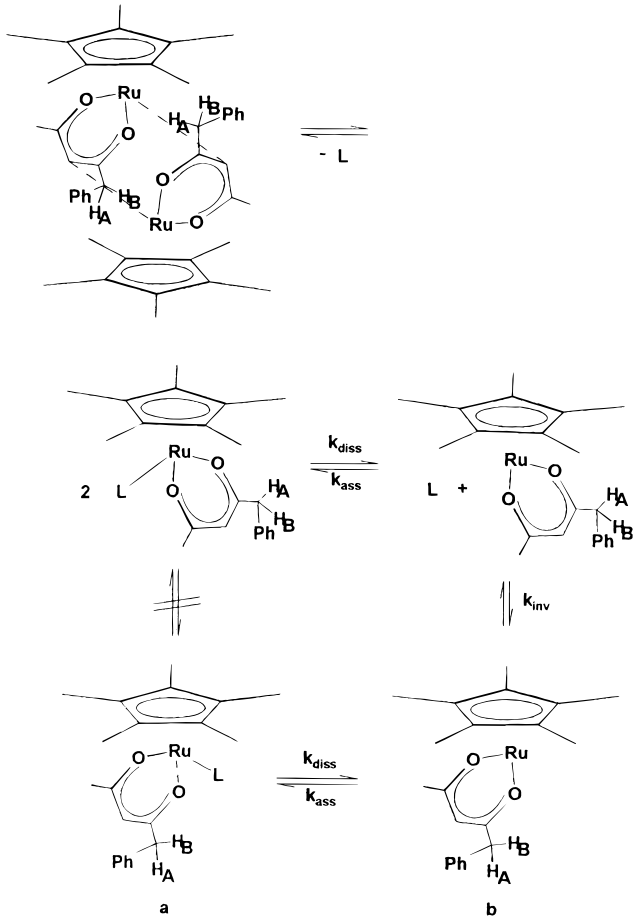

The dissociation−association steps involved in the interconversion of enantiomers of **3**·L are shown in Scheme 3. In the presence of a ligand L the (vertical) inversion equilibrium is coupled to a (horizontal) dissociation equilibrium. In order to conceptually distinguish both processes, inversion is depicted as a separate step, even though in reality it may be indefinitely fast, that is concomitant with the dissociation. In general the observable inversion barrier with rate constant k_{obsd}^{inv} will be influenced by the presence of L, since inversion can only occur in the unsaturated monomer.

Dissociation−association of L can be detected in the NMR either by changes in the ligand spectrum on complexation to the metal or, in case the ligand is present in excess, by separate signals for free and complexed ligand in the regime of slow exchange. Both criteria have been used to evaluate the dissociation-inversion kinetics of the adducts. An equilibrium constant $K_{ass.} > 1$ for adduct formation under conditions of rapid exchange at ambient temperature, which is the case for most of the σ-donor ligands, is evident from shifts of the NMR signals of dimers **2**-**2** and **3**-**3** on ligand addition. Since there is no free ligand signal for the 1:1 Ru−L mixture at low temperature (when slow exchange is obvious from split ligand signals), $K_{ass.}$ ($k_{ass.}/k_{diss.}$) appears to be ≫1 and is not easily determined

(8) (a) Fernández, J. M.; Gladysz, J. A. *Organometallics* **1989**, *8*, 207. (b) Dewey, M. A.; Knight, D. A.; Klein, D. P.; Arif, A. M.; Gladysz, J. A. *Inorg. Chem.* **1991**, *30*, 4995. (c) Knight, D. A.; Arif, A. M.; Gladysz, J. A. *Z. Naturforsch., B* **1992**, *47*, 1184. (d) Richter-Addo, G. B.; Knight, D. A.; Dewey, M. A.; Arif, A. M.; Gladysz, J. A. *J. Am. Chem. Soc.* **1993**, *115*, 11863.

Table 1. Chemical Shifts[a] of Adducts of 3

ligand	Cp*	Me	Bz	CH	*o*-phenyl	*m*-phenyl	*p*-phenyl	other
none (298 K)	1.597	1.92	3.52	5.20	7.25	7.16	7.07	
none (183 K)	1.38	2.04/2.02[b]	3.53/3.54	5.30	7.52/7.60	7.34/7.31	7.21/7.19	
PPh_3	1.15[c]	1.54	3.03/3.16	4.83	7.01		7.59	
CO	1.305	1.66	3.18	5.07	7.12			
THT·**3**	1.58	1.35	3.01/2.97	5.13	7.24	7.14	7.05	2.47 (α)/2.29 (β)
THT·**2**	1.62	1.85		4.05				
MeSEt	1.53	1.81	3.28[d]	5.10	7.00/6.95	6.81/6.82	6.72	1.22 (s), 1.0 (t) 1.98 (q)
DABCO	1.46	1.95	3.35[f]	5.25	7.25	7.13	7.05	2.28, 2.46/2.58[e]
p-Me-$C_6H_4S(O)Me$	1.255/1.275	1.79	3.183/3.150 3.185/3.120	5.09	7.02	6.92	6.84	7.88/7.93, 6.88/6.84, 2.13/2.23
3-cyanopyridine	1.48	1.82	3.354/3.078	4.83	7.26/7.19	7.23	7.14	8.71/8.0, 8.16/7.98 (d), 5.96/6.18 (d), 5.62/5.80 (t)
$HC{\equiv}CSiMe_3$	1.47	2.10/1.98	3.80/3.52[f]	5.23	7.56/7.50	7.31/7.28	7.16	

[a] In toluene-d_8; reference is $\delta(CD_2H-C_6D_5)$ 2.09. [b] Pairs of chemical shifts refer to low-temperature spectra and are given in the order major/minor diastereoisomer. [c] $^4J_{PH} = 1.45$ Hz. [d] Not resolved at low temperature; see text. [e] CH_2 of bisadduct and monoadduct, respectively. [f] Mean chemical shifts of two AB quartets.

Table 2. Activation Parameters for Ligand Exchange and acac Inversion in Adducts of 3

		E_a kJ/mol		$\Delta G^{\ddagger}_{273}$ kJ/mol	
ligand added to **3**	T_c, K	inversion	ligand exch	inversion	ligand exch
none	195	43.5 ± 0.7		33.2	
PPh_3	350	111.3	116.4	76.0	82.6
THT	233	55.2	95.5	41.8	42.1
DABCO	233	(44.2)[a]	48.1 ± 0.8	47.2	45.8
MeSEt	228	27.7[b]	32.7		47.1
p-Me-$C_6H_4S(O)Me$	273	55.5[a]	60.5[b,c]	56.2	56.3[c]
3-cyanopyridine	233	50.8	46.4	48.9	49.5

[a] From line shape of Cp* singlets. [b] From line shape of phenyl *o* protons. [c] Subject to larger uncertainty due to change in population and chemical shift over the temperature range where line shape changes.

by integration. In case the fraction of complexed L or **3** respectively changes appreciably with temperature, a sizeable shift of the corresponding NMR signals would result (the observed shift is the sum of $\delta_i x_i$), which was not observed. For $K_{ass.} \gg 1$, however, changes in K would no longer be obvious from NMR shifts. In this case a direct and independent determination of $k_{diss.}$ and $k_{ass.}$ is the only means for determining $K_{ass.}$.

The case of a rapid equilibrium, apparently slowed down by diminishing the fraction of the equilibrating species, has been treated in detail for the inversion of amines protonated to a large extent by adjusting the pH.[9,10] The observed inversion rate constant is related to the true rate constant k^{inv} simply as

$$k_{obsd}{}^{inv} = k^{inv}/K_{ass.} \qquad (2)$$

a relation which holds as long as $k_{obsd}{}^{inv} \gg k_{diss.}, k_{ass.}$.[10] This seems to be the case for most of the ligands dealt with below.

A further feature to be noted in Scheme 3 is the monomer−dimer equilibrium, which competes with the association equilibrium. Dimers should be formed as soon as the monomer concentration, as determined by the association equilibrium, exceeds that given by the monomer−dimer equilibrium. As a consequence, inversion barriers observed in the presence of L should never be lower than those found in pure toluene.

Table 2 collects activation parameters as E_a and as $\Delta G^{\ddagger}_{273}$ values. The former were obtained from Arrhenius plots, whereas the latter are extrapolations of Eyring plots to 273 K. $\Delta S^{\ddagger}$ values obtained from the temperature dependence of $\Delta G^{\ddagger}$ were small (±2−5 J/(mol K)) and were subject to greater uncertainty. They cannot be used as a basis for a mechanistic discussion.

The activation parameters are derived from first-order rate constants as inverse NMR lifetimes. To convert these into chemical rate constants as defined by Schemes 2 and 3, they have to be multiplied by a factor of 2, since on average every second dissociation event will interchange benzylic protons. This difference, however, does not influence E_a and consequently $\Delta G^{\ddagger}_{273}$, which depend only on the temperature dependence of k and not on its absolute value.

Symmetrical Bases. PPh_3. PPh_3 forms a stable adduct with **3** similar to the $P(OMe)_3$ adduct of **2**, which was characterized by X-ray structure analysis.[4] In the NMR benzylic protons appear as a sharp AB quartet at ambient temperature. Heating of a toluene solution of this adduct shows coalescence of the AB quartet at 80 °C. A virtual inversion barrier of 80.6 kJ/mol ($\Delta G^{\ddagger}$) at the coalescence temperature was found from the ^1H NMR line shape. A similar value (Table 2) was obtained from coalescing ^{31}P signals in a sample containing 1 mol of PPh_3 in excess. Since in that case phosphine exchange ($k \approx 70$ s^{-1} at 80 °C[11]) is 2 orders of magnitude slower than inversion (extrapolated as ∼7000 s^{-1} at 80 °C), the coalescence only measures the dissociation of the phosphine. The same conclusion is drawn from the similar values for $\Delta G^{\ddagger}$ and E_a for the two processes. The energy of activation can thus be equated to the enthalpy of phosphine dissociation, which roughly represents the binding energy of the phosphine to **3**.

CO. The CO adduct of **3** shows a single line for benzylic hydrogens at ambient temperature. Lowering the temperature causes this line to split into an AB quartet not by coalescence but by a temperature-dependent shift difference $\Delta\nu_{AB}$ that steadily increases with lower temperature, reaching a value of 70 Hz (at 500 MHz) at −100 °C. The AB coupling is not much different from that of the dimer. This peculiar behavior is only compatible with a fast, but strongly temperature-dependent, equilibrium. If this were a dissociation−association equilibrium, then from the apparent AB shift difference and under the assumption of complete

(9) Saunders, M.; Yamada, F. *J. Am. Chem. Soc.* **1963**, *85*, 1822.
(10) Delpuech, J.-J. *Org. Magn. Reson.* **1970**, *2*, 91.

(11) The rate of chemical exchange k_{ex} is twice that value, since only every second dissociation event causes magnetization transfer from bound to free phosphine and vice versa; cf.: Green, M. L. H.; Wong, L.-L.; Sella, A. *Organometallics* **1992**, *11*, 2660.

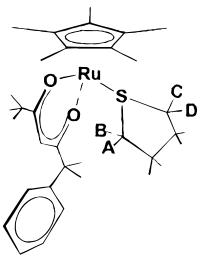

Figure 4. Preferred conformation of the tetrahydrothiophene ligand in **3**·THT, obtained through minimization of torsional energies.

adduct formation at −100 °C one would obtain only 15% adduct at −20 °C and 43% at −60 °C: that is, essentially complete dissociation at room temperature. (Values were simulated by interchanging the AB pattern rapidly with a singlet, i.e. a single chemical shift for both lines but no interchange of individual spins.) The conclusion is incompatible with the chemical behavior of the CO adduct, which can be recrystallized without decomposition. Moreover, the mean chemical shift $(\nu_A + \nu_B)/2$ is nearly temperature-independent but differs by 0.35 ppm from that of **3** in toluene (Table 1), which is incompatible with substantial dissociation. An alternative explanation would be a conformational equilibrium of the phenyl group with strongly temperature dependent site populations. An exchange constant of about 2000 s^{-1} at −40 °C is required to simulate the observed line width, and such a fast process is best accounted for by some internal motion. As a consequence, however, no dissociation or interconversion barrier could be determined because the AB shift difference has vanished at a temperature where onset of dissociation is to be expected. A relatively stable adduct can be inferred from sharp lines for the AB system up to 0 °C.

Tetrahydrothiophene (THT). Adduct formation of **3** with a ligand of at least C_s symmetry is indicated by an NMR pattern of lower symmetry in the limit of slow exchange. Thus, 1:1.05 mixture of **3** and THT (by NMR intergation) shows sharp signals for THT protons as well as protons of **3** at ambient temperature. Line broadening of α (δ 2.44) and β (δ 1.24) THT protons starts at −20 °C, and the signal finally splits into a 2:1:1 pattern for α and a broad, similar multiplet for β protons at −80 °C. Figure 4 shows a conformation of the adduct where the geometry of **3** from the X-ray structure was combined with a minimum conformation of THT from a modeling program.[12] In this structure the THT ligand and the phenyl group of **3** are rotated into minimum energy conformations, respectively. Assignment to the observed low-temperature multiplet would thus be as $H_A + H_D$:H_B:H_C. Note that, due to the pyramidal configuration at sulfur, exchange of H_A with of H_C and of H_B with H_D is only achieved by dissociation of THT, not by rotation around the Ru−S bond. The assignment is corroborated by a 1:1 splitting of the α-protons in the THT adduct of **2** at low temperature. In contrast to the case for sulfide adducts $[CpRe(NO)(PPh_3)SR_2]^+$,[13] we measure dissociation of sulfide rather than rotation and inversion at the sulfur atom. This is because in all cases where the ligand was added in excess, a single signal for the ligand groups occurs at ambient temperature, which is split into separate signals for complexed and free ligands at low temperature. This means that different signals for diastereotopic protons in the adduct are seen only if the exchange between free and coordinated ligand has become slow enough. The same reasoning is valid for the unsymmetrical sulfide MeSEt discussed below.

Simulation of the line shape for the α protons gave, for example, $k_{diss.} = 450\ s^{-1}$ at −50 °C. At this same temperature $k_{obsd}^{inv} \approx 50\ s^{-1}\ M^{-1}$,[14] which means, apparently, that inversion is still slower than association−dissociation. Applying eq 2 and inserting $k^{inv} = 7017\ s^{-1}$ as a lower limit, gives $K_{ass.} = k^{inv}/k_{obsd}^{inv} = 7017/50 = 140\ M^{-1}$, that is, an association equilibrium far toward the adduct.

Diaza[2.2.2]bicyclooctane (DABCO). In a toluene solution containing a 1:1.7 mixture of **3** and DABCO line broadening of the DABCO singlet starts at −20 °C. At −80 °C the signal has split into a sharp singlet for uncomplexed amine (δ 2.34) and three broad signals of unequal intensity for complexed amine assigned to the monoadduct (δ 2.57, 2.47) and the symmetrical bisadduct **3**·DABCO·**3** (δ 2.28). Concomitant with these splittings the Cp*, 3-Me, and all three phenyl multiplets are doubled in the same ratio (1:1.65) given by **3**·DABCO·**3**:**3**·DABCO. Benzylic protons appear as a single AB quartet, and also the methine proton of **3** is one singlet. Both seem to have accidentally identical shifts in both adducts. Chemical shifts δ_A and δ_B different from those of **3**-**3** in toluene again show that **3** is entirely incorporated into adducts with the amine. It is difficult in this case to determine the exchange rate of the amine due to two different, possibly temperature-dependent, equilibria involved. A qualitative estimate shows, however, that this exchange is rather fast and is in any case faster than the apparent inversion, which is considerably slowed down by amine complexation (Table 2).

Unsymmetrical Bases: Diastereoselective Adduct Formation. When the ligand added to **3** is prochiral, two new chiral centers at Ru and at the ligating atom are generated on adduct formation, giving rise to two diastereomeric pairs. Diastereoselectivity in adduct formation was evaluated with four unsymmetrical (prochiral) ligands: MeSEt, *p*-Me-C_6H_4S(Me)O, 3-cyanopyridine, and an alkyne, $Me_3SiC{\equiv}CH$. Diastereoisomers are visible in the NMR in the first two cases but do not show up in the cyanopyridine adduct and are not clearly distinguishable for the acetylene.

MeSEt. Due to the prochiral nature of the unsymmetrical sulfide, in principle four diastereoisomeric adducts can be formed. LT NMR spectra containing **3** and S(Me)Et in the ratio 1:1.14 show *two* diastereoisomers in the ratio 1:0.7, visible from, e.g., the two doublets of the phenylic ortho protons (Table 1) or the two methyl triplets of the S−Et group. This is to be expected, since only in one of the two possible orientations of the sulfide is the lone pair positioned for adduct formation.

Benzylic protons start line broadening at −20 °C and appear as a partially resolved AB quartet with a very small shift difference ($\Delta\nu_{AB} \cong 0.03$ ppm) at −50 °C.

(12) Höveler, U. *Moby*; University of Münster, Springer 1992.
(13) Méndez, N. Q.; Arif, A. M.; Gladysz, J. A. *Organometallics* **1991**, *10*, 2199.
(14) k_{obsd}^{inv} is a second-order rate constant; thus, the inverse lifetime as determined from NMR has to be divided through the ligand concentration (about 0.1 M) to convert it to k_{obsd}^{inv}.

Below −60 °C the signals broaden again and at −80 °C appear as two AB quartets. Chemical shifts at ambient and low temperature are different from those of **3**-**3** in toluene. Thus, most of the Ru complex is present as the sulfide adduct. Simulating line broadening of the *o*-protons and of the Me triplets yields activation energies around 30 kJ/mol. Though these figures are not very precise in this case, they nevertheless prove an association equilibrium faster than the inversion without extra ligand present. It appears that, notwithstanding a more mobile association−dissociation equilibrium, the virtual inversion can still be slower than in the dimer. The peculiar temperature-dependent behavior of the benzylic protons points to the existence of two processes with different activation energies (not resolved explicitly in the experiment). One slows down inversion and the second one, operative at still lower temperature, causes splitting into diastereoisomers. The point is further discussed below.

***p*-Me-C_6H_4S(Me)O.** The sulfoxide was added to the toluene solution of **3** as the pure *S* enantiomer to obtain a **3**:*p*-Me-C_6H_4S(Me)O ratio of 1:1.4. Signal broadening is already obvious for some signals at ambient temperature. All signals broaden below 20 °C and are sharp again at −45 °C. At this temperature the S(O)Me group and, most noticeably, the ortho protons from the sulfoxide arene around δ 7.9 have separated into three sets, assigned to the two diastereoisomeric adducts R_{Ru} and S_{Ru} and the signal for the uncomplexed ligand. In the same manner were Cp* and Me singlets from **3** split into two signals, each of intensity ratio 1:0.45 (at −45 °C). Benzylic protons, at −45 °C, appear as two sharp AB quartets of unequal intensity with chemical shifts and intensity ratios distinctly different from those of **3** in toluene. Temperature-dependent line shapes of the different groups were simulated, and the resulting *k* values were found close enough to ascertain the same process as being responsible for all line shape changes. The value for E_a given in Table 2 has been obtained by simulating the line shape of the Cp* signal. It also became obvious during the simulation that intensity ratios had to be changed for different temperatures, being closer to 1 at higher temperature. The ratio change in the temperature interval where separate signals are seen for e.g. the Cp* group (−45 to −15 °C) is, however, too small to allow thermodynamic parameters for the equilibrium of diastereoisomers to be determined.

3-Cyanopyridine. The LT NMR of a solution containing **3** and 3-cyanopyridine in the ratio 1:1.23 shows two sets of pyridine signals in a corresponding ratio with relatively large displacements, assigned to complexed and free pyridine. Benzylic protons are split into a single AB quartet; aromatic protons from the Phacac ligand are not subject to any temperature-dependent line broadening in this case. Moreover, Me and Cp* signals remain singlets down to low temperature. This means that the ligand gives rise to one single diastereoisomer only, or more realistic, to two diasteromers still rapidly interconverting at low temperature through rotation around the Ru−N bond. The existence of a sharp AB quartet, on the other hand, shows that the process occurs without Ru−N bond cleavage. The first-order pyridine exchange rate and the rate of acac inversion have been found to be not much different from one another in the temperature interval of slow to medium exchange.

$Me_3SiC{\equiv}CH$. In the case of this unsymmetrical acetylene, adduct formation is less easy to prove. When the acetylene is added in about 3-fold excess, the Me_3Si singlet at δ 0.28 starts to broaden from −20 °C but exchange is slow only at −50 °C, at which point separate signals for complexed and free acetylene have developed. Since the chemical shift of the free acetylene Me_3Si group has undergone only a minor change between ambient and low temperature (and in the wrong direction, i.e. downfield), it must be concluded that association equilibrium at ambient temperature is not only fast but also to a larger extent is shifted toward the free complex: that is, **3**-**3**. Consequently, line broadening of the benzylic singlet starts at the same temperature as in neat toluene but much lower temperature is needed for individual lines to reappear. The spectrum at −90 °C, though not yet sharp in the benzyl region, shows a pattern similar to that of the diastereoisomeric pair of dimers of **3** in toluene, but with additional peaks for an acetylene adduct. Two methyl signals of unequal intensity for complexed acetylene around δ 0.44 at this temperature can be interpreted as originating from two orientations of the acetylene with respect to the benzyl group in the adduct. From line broadening of the ortho protons the activation energy E_a = 18 kJ/mol can be estimated for the inversion of the acac ligand, which is much lower than the value found for the dimer in toluene. In this case the adduct seems to be rather weak and to compete with the dimer.

Discussion

Addition of two-electron-donor ligands L to the solutions of the dimers **2**-**2** and **3**-**3** in all cases cleaves them into monomeric adducts (**2**,**3**)·L. This occurs with π-acceptor as well as with pure σ-donor ligands. The adducts are, however, of widely differing stability, ranging from isolable compounds for phosphines, phosphites, and CO to solution species, whose formation is evident from the influence of added ligand on the inversion rate of the dimer.

Due to a number of shortcomings, such as chemical shifts and equilibrium populations varying with temperature, which cannot be evaluated above coalescence temperature, some of the activation parameters E_a and $\Delta G^{\ddagger}_{273}$ in Table 2 pertaining to ligand association can bear a greater uncertainty which is not reflected in the standard deviation of the Arrhenius plots and are believed to be realistic within 5−10%. Bearing in mind these uncertainties, it still follows from Table 2 unambiguously that for the ligand MeSEt not only the association equilibrium but also the inversion, measured in that case from line broadening of phenylic ortho protons, is faster than for the pure dimer (E_a is below the value of the dimer in pure toluene). The same is true for the $Me_3SiC{\equiv}CH$ adduct, where E_a has been found from ortho proton line broadening as low as about 18 kJ/mol. The situation arises if, in spite of an equilibrium shifted toward the adduct **3**·L, the latter is kinetically still very fast. This fact arises because the observed NMR lifetime is determined by the faster of the two competing equilibria, adduct formation−dissociation or dimerization. This will hold as long as the inversion in the monomer is much faster than either

Table 3. NMR Shifts of Complexes [Cp*Ru(η^2-OC(R^1)CR^3C(R^2)O)]$_n$ and Cp*Ru(η^2-OC(R^1)CHC(R^2)O)L

R^1, R^2, R^3	Cp*	CH (R^3)	R^1 R^2
OEt, OEt, H (**6a**)[a]	1.62	5.15	4.09 (q), 1.18(t)
OEt, OEt, H (**6b**)[a]	1.67	3.03	3.88 (q), 0.87(t)
Me, Me, Bz[b]	1.66	3.38 (s), 7.01 (m), 7.16 (m)	1.97 (s)
Me, OEt, H[a]	1.61	5.07	2.01 (s), 4.17 (q), 1.17 (t)
Me, Ph, H[b]	1.68	5.85	2.10 (s)
Me, CF_3, H[a]	1.58, 2.15 (q), 0.87 (t)[c]	5.65	2.01
R^1 R^2 R^3 L	Cp*	CH (R^3)	R^1, R^2
Me, OEt, H,[d] $P(OMe)_3$	1.64 (t, $^4J_{PH}$ = 2.6 Hz)	4.96	3.46 ($P(OMe)_3$), 2.66 (Me), 4.36, 1.26 (OEt)
OEt, OEt, H, PPh_3	1.38 (d) ($^4J_{PH}$ = 1.45 Hz)	4.65	3.90, 0.94 (OEt)
Me, Ph, H, PPh_3[b]	1.42 (d) ($^4J_{PH}$ = 0.6 Hz)	5.60	1.73
Me, Ph, H, PMe_3[b]	1.56 (d) ($^4J_{PH}$ = 1.6 Hz)	5.83	1.86
Me, Ph, H, CO[b]	1.54	5.92	1.92
Me, Bz, H, PMe_3[e]	1.44 (d) ($^4J_{PH}$ = 1.7 Hz)	5.10	3.25 (CH_2), 1.73 (CMe), 1.11 (PMe)

[a] In C_6D_{12}. [b] In C_6D_6. [c] Cp ligand is C_5Me_4Et. [d] According to NMR the complex is Cp*Ru(η^1-OC(Me)CHCOOEt)($P(OMe)_3$)$_2$. [e] In CD_3COCD_3.

one of these processes. The existence of a thermodynamically favored (over dimer formation) but kinetically labile adduct explains the benzyl singlet in **3**·PMe_3 at ambient temperature as well as the rapid inversion of **3-3** at low temperature found in THF. In the latter case the adduct **3**·THF, though thermodynamically favored, must be kinetically particularly labile in order to counterbalance the high concentration of solvent (about 10 M) with respect to complex.

We finally turn to the two consecutive processes observed in the case of MeSEt as ligand, when the temperature was lowered. A single, partially developed AB quartet at −60 °C means slow inversion at this temperature. Since the chemical shift of this AB quartet is quite different from that observed for the dimers **3-3** (Table 1), it seems clear that the splitting at this temperature refers to the adduct **3**·S(Me)Et. At this temperature, however, dissociation of the adduct must still be rapid, since separate patterns for individual diastereoisomers, such as splitting of the ligand signals, occur only at still lower temperature. The AB pattern at −60 °C is reproduced with an inversion rate constant of about 10 s^{-1}, whereas from the difference of chemical shifts of the two AB quartets at −90 °C a rate constant $k > 50$ s^{-1} is calculated as being necessary for coalescence of these quartets. In other words, a sulfide molecule must have a chance to dissociate and reassociate with Me and Et groups interchanged without inversion of the acac ligand occurring. This in turn means a finite lifetime of the coordinatively unsaturated pyramidal species as depicted in Scheme 3.

Our quantum-chemical calculations on the model compound CpRu(acac) revealed a very shallow minimum for the pyramidal C_s as compared to the straight C_{2v} conformation. In fact, the stabilization of the 16-VE pyramidal species calculated for $CpMn(CO)_2$ by Hofmann[15] and verified experimentally for CpRe(NO)-PPh_3^+ by Gladysz and co-workers[8] is counteracted if the ligands are σ-donors and in particular π-donors instead of acceptors, a fact already obvious at the EHT level.

The relatively weak intermolecular binding within the dimers is reflected not only in the long Ru−C7 distance as discussed above but also in the very small coordination shift of C7 in the ^{13}C NMR. Thus, in **2-2** C7 resonates at 95.4 ppm, which can be compared to monomeric acac complexes of Ru^{II} such as (COD)Ru-(acac)$_2$[16] (98.8 ppm) or **3**·CO (98.78 ppm) (C_6D_6 for all). The small energy of dimerization ensures that **2-2** and **3-3** are convenient sources of the coordinatively unsaturated monomers for all practical preparative purposes.

(15) Hofmann, P. *Angew. Chem., Int. Ed. Engl.* **1977**, *16*, 536.

Table 4. Crystallographic Data, Collection Parameters, and Refinement Results for 3

empirical formula	$(C_{21}H_{26}O_2Ru)_2$
fw	823.02
diffractometer	Enraf-Nonius CAD4
cryst color	dark red
cryst shape	irregular
cryst dimens (mm)	ca. 0.3 × 0.3 × 0.3
cryst syst	triclinic
space group	$P\bar{1}$ (No. 2)
a (Å)	9.580(1)
b (Å)	10.336(1)
c (Å)	11.003(1)
α (deg)	100.63(1)
β (deg)	110.71(1)
γ (deg)	103.176(9)
V (Å^3)	949.28
Z	2.5
D_{calcd} (g/cm^3)	1.440
F_{000}	424
μ(Mo Kα) (cm^{-1})	8.2
scan type	$\omega/2\theta$
temp (K)	298
no. of unique rflns	4321
no. of obsd rflns ($I > 2\sigma(I)$)	4113
no. of params in refinement	218
R	0.026
R_w	0.028

Experimental Section

Preparation of acac complexes was done with anhydrous, nitrogen-saturated solvents under nitrogen using conventional Schlenk techniques. NMR spectra were recorded at 500 MHz proton frequency on a Varian Unity 500 instrument. Temperature calibration was done with methanol. Line shape simulations were performed with the GEM-NMR[17] or the DNMR5[18] program. Line shapes of the two overlapping AB quartets of **3** were kindly simulated by Dr. H. Brussaard at the University of Nijmegen.

Preparation of 2 from [Cp*$RuCl_2$]$_2$. The heterogeneous mixture of 0.224 g (0.37 mmol) of [Cp*$RuCl_2$]$_2$, 1 g of anhydrous K_2CO_3, and 78 mg (0.74 mmol) of acacH in 20 mL of 2-propanol

(16) Koelle, U.; Flunkert, G.; Görissen, R.; Schmidt, M. U.; Englert, U. *Angew. Chem., Int. Ed. Engl.* **1992**, *31*, 440.

(17) A version of GEM NMR by U. Seimet, University of Kaiserslautern, was kindly provided by Dr. C. G. Kreiter, University of Kaiserslautern.

(18) A PC version of DNMR 5 was kindly provided by Dr. H. Wadepol, University of Heidelberg.

was stirred overnight at ambient temperature, whence the color changes from brown to red. 2-Propanol was stripped *in vacuo*; the dry residue was extracted with several 10 mL portions of pentane, giving a red solution. When it was cooled to −78 °C, the concentrated pentane solution gave 0.23 g (94%) of red needles. ^{1}H NMR (C_6D_6): δ 1.64 (s, 15 H), 1.95 (s, 6 H), 5.11 (s, 1 H).

Complexes **3**−**8** were prepared by adding a stoichiometric amount of the pentanedionate to a solution of **1** in pentane. After 1 h at ambient temperature the solutions were concentrated to a small volume. When they were cooled to −78 °C, the products crystallized as red needles or plates. Yields depend on the solubility and are nearly quantitative for the less soluble derivatives. Complexes were characterized by NMR, MS, and in a few cases by elemental analysis. For NMR data, see Table 3.

3: Anal. Calcd for $C_{21}H_{26}O_2Ru$ (M_r 411.5): C, 61.29; H, 6.37. Found: C, 61.07; H, 6.31. **6a**/**6b**: Anal. Calcd for $C_{17}H_{26}O_4Ru$ (M_r 395.4): C, 51.63; H, 6.63. Found: C, 51.33; H, 6.67. **8a**/**8b**: ^{1}H NMR (C_6D_6) δ 1.03/0.97 (d, $^4J_{PH}$ = 1.6 Hz, Cp*), 0.31, 0.33, 0.564 (s, Me), 2.39/2.48 (m, CH), 1.38 (m, CH_2), 0.85 (m, CH_2), 7.42/7.07 (m, *m* phenyl), 6.8 (m, *o*,*p* phenyl); ^{13}C NMR (C_6D_6) δ 9.24 (Cp*), 8.45, 17.88, 20.01 (Me), 27.99, 29.76 (CH_2), 48.98 (*C*H), 47.66, 48.9, 50.1, 57.6, 57.9 (bridge and bridgehead C), 114.9, 203.1 (O*C*), 161.3, 117.2, 111.7 (*C*F); ^{31}P NMR δ 41.11/42.01.

X-ray Structure Determination of 3. A single crystal of suitable quality was grown from pentane. The crystal was sealed in a glass capillary under a protecting argon atmosphere. Data were collected at room temperature. Details of the X-ray structure determination are listed in Table 4. The solid-state structure of **3** is shown in Figure 1, and selected structural parameters are listed in the figure caption. The structure was solved by the heavy-atom method, employing the Fourier routine of the XTAL3.2[19] package of crystallographic programs.

Supporting Information Available: Tables giving X-ray experimental details, positional and thermal parameters, bond distances and angles, and dihedral angles for **3** (15 pages). Ordering information is given on any current masthead page.

OM960718G

(19) Hall, S. R.; Flack, H. D.; Stewart, J. M. *XTAL3.2 Reference Manual*, Universities of Western Australia, Geneva, and Maryland, 1992.